
Towards Improving Learning from Demonstration Algorithms via MCMC Methods

Hanwen Qi, Edward Sun, Harry Zhang

Abstract

Behavioral cloning, or more broadly, learning from demonstrations (LfD) is a promising direction for robot policy learning in complex scenarios. Albeit being straightforward to implement and data-efficient, behavioral cloning has its own drawbacks, limiting its efficacy in real robot setups. In this work, we take one step towards improving learning from demonstration algorithms by leveraging implicit energy-based policy models. Results suggest that in selected complex robot policy learning scenarios, treating supervised policy learning with an implicit model generally performs better, on average, than commonly used neural network-based explicit models, especially in the cases of approximating potentially discontinuous and multimodal functions.

1 Introduction

Learning from demonstration (LfD) has been an active topic in robotics research. In the context of robotics and automation, learning from demonstration (LfD) is the paradigm in which robots acquire new skills by learning to imitate an expert. Among a variety of LfD algorithms, behavioral cloning (BC) Pomerleau [1998] remains one of the most straightforward methods to acquire skills in the real world where the robotic agent tries to imitate (i.e. clone) an expert policy via supervised learning. Despite its simple problem formulation and significant inductive bias acquired from supervised learning methods, the method has valid both empirical and theoretical shortcomings such as sample inefficiency and distribution shift in inference time Ross et al. [2011], Tu et al. [2021], in practice it enables some of the most compelling results of real robots generalizing complex behaviors to new unstructured scenarios Zhang et al. [2018], Florence et al. [2019], Zhang et al. [2021]. The choice of LfD over other robot learning methods is compelling when ideal behavior can be neither easily scripted (as is done in traditional robot programming) nor easily defined as an optimization problem, but can be demonstrated. In this project we tackle the topic from a probabilistic point of view, where we investigate the effect of novel sampling techniques in learning from demonstration. This work is inspired by recent investigation and advancement in the field of LfD using implicit models Avigal et al. [2021], Du and Mordatch [2019], Du et al. [2020], where the BC problem is reformulated as an implicit function calculated with an energy-based model via:

$$\hat{a} = \operatorname{argmin}_{a \in \mathcal{A}} E_{\theta}(o, a) \text{ instead of } \hat{a} = \pi_{\theta}(o).$$

With the introduction of this implicit energy-based policy, we would need to intelligently sample from this function in order to produce on-policy samples during training and test time. Thus, we investigate how implicit function with different probabilistic sampling methods would improve the usual behavioral cloning/imitation learning performance. We conduct experiments in complex simulated environments that both naive BC and naive RL policy such as DDPG and SAC would fail Haarnoja et al. [2018], Hou et al. [2017]. Results suggest that this simple change can lead to remarkable improvements in performance across a wide range of contact-rich tasks such as deformable objects manipulation, especially simulated dough manipulation tasks.

The contribution of our work is three-fold:

1. A comprehensive evaluation of various sampling methods in LfD algorithms.
2. Simulated experiments that compare regular policy learning vs. energy-model-based implicit policy learning.
3. A sufficiently complex simulated platform for deformable objects manipulation that could be used as a test bed for other LfD algorithms.

2 Related Work

Learning from Demonstrations. Learning from demonstrations, or often interchangeably, imitation learning, is a prevalent method in the field of robot learning Pomerleau [1998], Zhang [2016]. In addition, data-driving methods such as Peng et al. [2018], Ross et al. [2011], Zhang et al. [2020] combined with existing BC or RL methods have shown great potential in complex robotic tasks. Generative distribution-matching algorithms such as Ho and Ermon [2016], Zhang et al. [2021] require no labeling, but may require millions of on-policy environment interactions, which is expensive to collect in real robot setups. Other methods such as Kumar et al. [2020], Fu et al. [2020], Eisner et al. [2022] attempt to leverage both the abundance of pre-collected or offline data and the generalizability and flexibility of online value function-based policy learning in regular RL setup and come up with offline RL algorithms. Offline RL algorithms often show competitive performance that is even superior to expert demonstration performance. Perhaps the success of BC comes from its simplicity: it has the lowest data collection requirements, can be data-efficient Ross et al. [2011], Avigal et al. [2020], and is arguably the simplest to implement and easiest to tune due to the lack of hyperparameters.

Energy-Based Models and Implicit Policy Learning. LeCun et al. [2006], Song and Kingma [2021], Devgon et al. [2020], Avigal et al. [2020] provide a comprehensive overview of how energy-based models are formulated and trained. Energy-based models are chosen in many scenarios due to the desirable properties of out-of-distribution generalization and long-horizon sequential prediction Du et al. [2020], Sim et al. [2019] and discontinuity modeling Florence et al. [2021], Elmquist et al. [2022]. When used in robot learning tasks, EBMs with implicit policy learning are shown to outperform traditional explicit policies in a variety of tasks such as contact-rich pushing and placing, deformable objects manipulation, and door opening Florence et al. [2021], Eisner et al. [2022]. Moreover, the flexibility of MCMC sampling and EBMs also facilitates their prevalence in other domains such as computer vision tasks and text generation tasks Gustafsson et al. [2020], Deng et al. [2020], Pan et al. [2022]. In reinforcement learning, Haarnoja et al. [2017a], Zhang et al. [2023] uses an EBM formulation as the policy representation. Other recent work Du et al. [2020], Jin et al. [2024] uses EBMs in a model-based planning framework, or uses EBMs in imitation learning but with an on-policy algorithm. Another line of recent RL works has emerged to utilize an EBM as part of an overall policy Kostrikov et al. [2021], Nachum and Yang [2021], Shen et al. [2024].

Data-driven Deformable Objects Manipulation Methods. Due to the difficulties with defining a deformable object’s state representation, prior works have developed data-driven methods to learn from examples. Prior works mainly use the available data in two ways. One way is to leverage the available data to train a dynamics model and later use it for planning. Some train a particle-based dynamics model Li et al. [2019], Lin et al. [2021], Yao et al. [2023], some train a visual dynamics model Hoque et al. [2020], Lim et al. [2021, 2022], and others train a latent dynamics model Ma et al. [2021], Matl and Bajcsy [2021]. Among the model-based approaches, DPI-Net Li et al. [2019], Teng et al. [2024] is the most related to modeling elastic/plastic objects like dough.

As deformable object manipulation becomes increasingly popular, the need for training data result in many high-quality simulators Hu et al. [2020], Lin et al. [2020], Heiden et al. [2021], Huang et al. [2021]. We choose PlasticineLab Huang et al. [2021], which uses Material Point Method Hu et al. [2018] to model elastoplastic material. The simulator is built on top of the DiffTaichi system Hu et al. [2020], which supports differentiable physics that allow us to perform gradient-based trajectory optimization.

Trajectory optimization

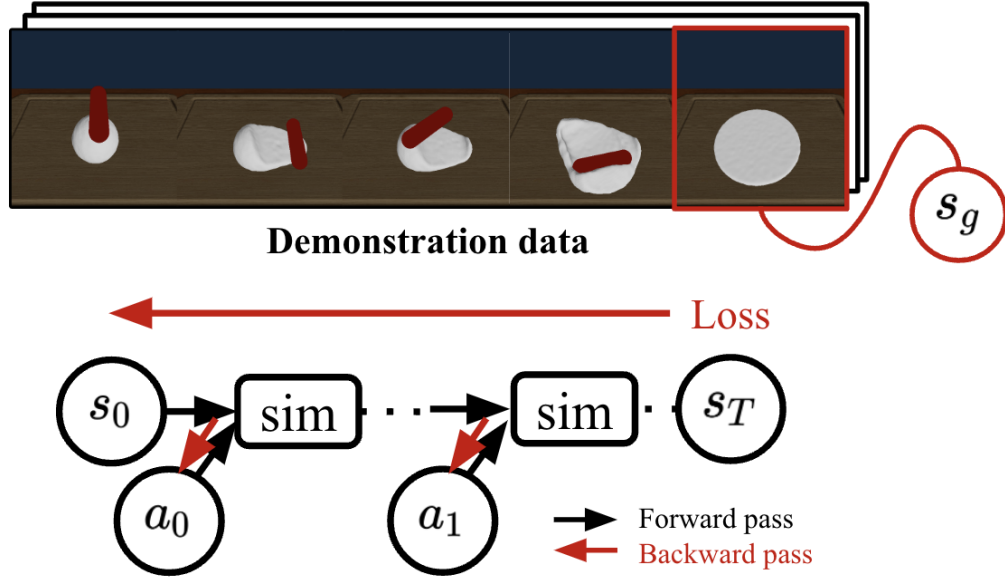


Figure 1: We perform trajectory optimization to obtain expert demonstrations. We first compute the loss between a target state and the states in our trajectory. We then back-propagate the gradient from the target shape through a differentiable simulator to get the updated actions.

3 Background

3.1 Markov Decision Process

A Markov Decision Process (MDP) is defined using the tuple: $\mathcal{M} = \mathcal{S}, \mathcal{R}, \mathcal{A}, \mathcal{O}, \mathcal{P}, \rho_0, \gamma$. \mathcal{S}, \mathcal{A} , and \mathcal{O} represent the state, action, and observation space. $\mathcal{R} : \mathcal{S} \times \mathcal{A} \rightarrow \mathcal{R}$ is the reward function. $\mathcal{P} : \mathcal{S} \times \mathcal{A} \rightarrow \mathcal{S}$ is the transition dynamics. ρ_0 is the probability distribution over initial states and $\rho_0 = [0, 1)$ is a discount factor. Let $\pi : \mathcal{S} \rightarrow \mathcal{A}$ be a policy which maps states to actions. In the partially observable case, at each time t , the policy maps a partial observation o_t of the environment to an action $a_t = \pi(o_t)$. Our goal is to learn a policy that maximizes the expected cumulative rewards $\mathbb{E}_\pi[\sum_{t=0}^{\infty} \gamma^t r_t]$, where r_t is the reward at time t . The Q-function of the policy for a state-action pair is $Q(s, a) = \mathcal{R}(s, a) + \gamma \mathbb{E}_{s', \pi}[\sum_{t=0}^{\infty} \gamma^t r_t | s_0 = s']$ where s' represents the next state of taking action a in state s according to the transition dynamics.

3.2 Imitation Learning

We consider the framework of Markov Decision Processes (MDP). We assume an infinite horizon setting. At any given state $s \in \mathcal{S}$, an agent makes decisions via a stochastic policy $\pi : \mathcal{S} \times \mathcal{A} \rightarrow \mathbb{R}_{\geq 0}$. We denote a trajectory to be a sequence of state-action pairs $\tau = (s_0, a_0, s_1, a_1, \dots)$. Any policy π , along with MDP parameters, induces a distribution over trajectories, which can be expressed as $p_\pi(\tau) = p(s_0) \prod_{t=0}^{\infty} \pi(a_t | s_t) \mathcal{T}(s_{t+1} | s_t, a_t)$. The return of a trajectory is the discounted sum of rewards $R(\tau) = \sum_{t=0}^{\infty} \gamma^t r(s_t, a_t)$.

In imitation learning, we sidestep the availability of the reward function. Instead, we have access to a finite set of D trajectories τ_E (a.k.a. demonstrations) that are sampled from an expert policy π_E . Every trajectory $\tau \in \tau_E$ consists of a finite-length sequence of state and action pairs $\tau = (s_0, a_0, s_1, a_1, \dots)$, where $s_0 \sim p_0(s)$, $a_t \sim \pi_E(\cdot | s_t)$, and $s_{t+1} \sim \mathcal{T}(\cdot | s_t, a_t)$. Our goal is to learn a parameterized policy π_θ which best approximates the expert policy given access to τ_E .

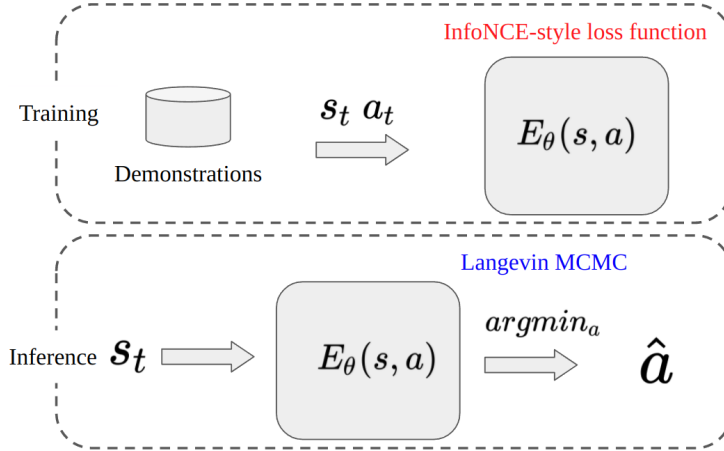


Figure 2: Baseline method: Implicit Behavioral Cloning. The energy-based model over states and actions is trained via an InfoNCE-style loss function. The inference is done by a MCMC sampling-based optimization procedure.

3.3 Behavioral Cloning

Behavioral cloning (BC) casts imitation learning as a supervised learning problem over state-action pairs provided in the expert demonstrations. In particular, we learn the policy by solving a regression problem with states s_t and actions a_t as the features and target labels respectively. Formally, we minimize the following objective:

$$\ell_{BC}(\theta) := \sum_{(s_t, a_t) \in \tau_E} \|a_t - \pi_\theta(s_t)\|_2^2. \quad (1)$$

Probabilistically, the BC problem can also be framed as optimizing the log-likelihood of the expert trajectories:

$$\ell_{BC}(\theta) := -\log \left(\sum_{i=1}^N P_\theta(\tau_i) \right) \quad (2)$$

where P_θ is a (learned) function modeling the probabilistic distribution of the expert demonstration data. Common choice of the P_θ model is a normal distribution defined as:

$$P_\theta(s_t, a_t) \propto \mathcal{N}(\mu_\theta(s_t), \sigma_\theta(s_t))$$

3.4 Implicit Behavioral Cloning

While the aforementioned methods explicitly solves for the BC objective function to learn a policy that takes as input a state and outputs an action, Implicit Behavioral Cloning [Florence et al., 2021] formulates BC using implicit models – specifically, the composition of $\arg \min$ with a continuous energy function E_θ to represent the policy π_θ :

$$\hat{a} = \arg \min_{a \in \mathcal{A}} E_\theta(s, a) \quad (3)$$

This formulates imitation learning as a conditional energy-based modeling (EBM) problem. During training, an energy model over the state and actions $E_\theta(s, a)$ are trained and at inference time (given s) performs implicit regression by optimizing for the optimal action \hat{a} via sampling or gradient descent. Existing literature [Florence et al., 2021] claims that implicit models outperform explicit model in modeling discontinuity and generalization.

4 Method

4.1 Generate Demonstrations by Trajectory Optimization

To generate demonstrations for rolling, we leverage a gradient-based trajectory optimization with the differentiable simulator. We write our trajectory optimization in Direct Shooting form Tedrake [2022] with all the constraints captured by the dynamics of the environment. Thus, given the initial state s_0 , the objective is:

$$\min_{a_1, \dots, a_T} L_{traj} = \sum_{t=0}^T L_t^{task} + \lambda L_t^{contact} \quad (4)$$

$$= \sum_{t=0}^T d(s_t, s_g) + \lambda s_t \quad (5)$$

$$\text{s.t. } s_{t+1} = \mathcal{T}(s_t, a_t) \quad (6)$$

where s_t, s_g are the current state and goal state, d measures the similarity between the current state and the goal state, $L^{contact}$ encourages the robot to make contact to the object, and λ weighs the different loss terms.

With differentiable dynamics, we can compute the gradient of the loss w.r.t the actions as follows:

$$\frac{\partial L_{traj}}{\partial a_t} = \sum_{t'=t+1}^T \frac{\partial (L_t^{task} + \lambda L_t^{contact})}{\partial s_{t'}} \frac{\partial s_{t'}}{\partial a_t} \quad (7)$$

where both L_t^{roll} and $L_t^{contact}$ are differentiable w.r.t. the ground-truth state s_t , and $\frac{\partial s_{t'}}{\partial a_t}$ can be computed efficiently via the back-propagation technique using the differentiable dynamics model. Therefore, a straightforward approach used by many others Huang et al. [2021], Li et al. [2019] is to use gradient-descent to directly update the actions, as shown in Figure 1.

4.2 Energy-based Policy Learning

As described in Sec. 3.4, we define a energy-based policy as the composition of arg min with a continuous energy function E_θ .

Given a dataset of expert demonstration $\{o_i, a_i\}$, where s_i and a_i are the observation and action at time step i , we use Noise Contrastive Estimation (NCE) to train the energy model. We assume the actions are n -dimensional and bounded by $a_{\min}, a_{\max} \in \mathbb{R}^n$. More specifically, we follow recent literature in energy model training and use InfoNCE Oord et al. [2018] loss.

InfoNCE loss (Eq. 8) can be seen as using cross-entropy loss to identify the positive action amongst a set of noise samples. To construct a training pair, we sample a tuple of demonstration (o_i, a_i) from the dataset, where a_i is the expert action. Then we sample N_{neg} negative actions $\{\tilde{a}_i^j\}_{j=1}^{N_{\text{neg}}}$ drawn from some proposal distribution. The specific type of proposal distribution will be described in the later sections. $e^{-E_\theta(o_i, \mathbf{a}_i)} + \sum_{j=1}^{N_{\text{neg}}} e^{-E_\theta(o_i, \tilde{\mathbf{a}}_i^j)}$ can be seen as an approximation of the partition function $Z(o_i, \theta)$, and larger N_{neg} always leads to more stable training.

$$\mathcal{L}_{\text{InfoNCE}} = \sum_{i=1}^N -\log(\tilde{p}_\theta(\mathbf{a}_i | o_i, \{\tilde{\mathbf{a}}_i^j\}_{j=1}^{N_{\text{neg}}})) \quad (8)$$

$$\tilde{p}_\theta(\mathbf{a}_i | o_i, \{\tilde{\mathbf{a}}_i^j\}_{j=1}^{N_{\text{neg}}}) = \frac{e^{-E_\theta(o_i, \mathbf{a}_i)}}{e^{-E_\theta(o_i, \mathbf{a}_i)} + \sum_{j=1}^{N_{\text{neg}}} e^{-E_\theta(o_i, \tilde{\mathbf{a}}_i^j)}} \quad (9)$$

In the following sections, we will describe two methods for inference and the corresponding proposal distribution for negative samples during training.

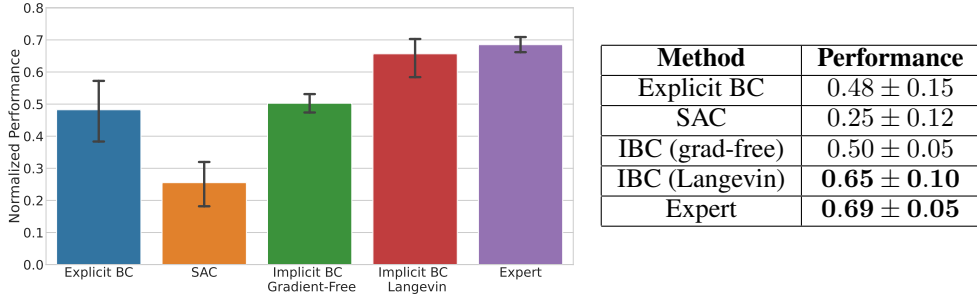


Figure 3: Normalized performance on 10 held out configurations.

4.2.1 Gradient-free Optimization

Training. We assume the actions are bounded and sample the negative samples from uniform distribution $\tilde{\mathbf{a}} \sim \mathcal{U}(\mathbf{a}_{\min}, \mathbf{a}_{\max})$, where $\mathbf{a}_{\min}, \mathbf{a}_{\max} \in \mathbb{R}^m$. To compute $\mathcal{L}_{\text{InfoNCE}}$, we use a batch size (N) of 100 with 256 negative examples per sample.

Inference. During test-time, given a trained energy model $E_{\theta}(\mathbf{x}, \mathbf{y})$, we use a simple gradient-free optimization method to get the action with lowest energy. The algorithm below is very similar to Cross-entropy Method (CEM) except that we use Expectation-Maximization (EM) algorithm to fit a Gaussian Mixture Model (GMM) to capture the multimodality of optimal action.

Algorithm 1: Derivative-Free Optimizer

Initialize: $\{\tilde{\mathbf{y}}_i\}_{i=1}^{N_{\text{samples}}} \sim \mathcal{U}(\mathbf{a}_{\min}, \mathbf{a}_{\max}), \sigma = \sigma_{\text{init}}$;
for iter in 1 to N_{iters} **do**
 $\{E_i\}_{i=1}^{N_{\text{samples}}} = \{E_{\theta}(\mathbf{x}, \tilde{\mathbf{y}}_i)\}_{i=1}^{N_{\text{samples}}}$ (compute energies);
 $\{\tilde{p}_i\}_{i=1}^{N_{\text{samples}}} = \left\{ \frac{e^{-E_i}}{\sum_{j=1}^{N_{\text{samples}}} e^{-E_j}} \right\}$ (use softmax to compute probability);
 $\{\tilde{\mathbf{y}}_i\}_{i=1}^{N_{\text{samples}}} \leftarrow \sim \text{GMM}(N_{\text{samples}}, \{\tilde{p}_i\}_{i=1}^{N_{\text{samples}}}, \{\tilde{\mathbf{a}}_i\}_{i=1}^{N_{\text{samples}}})$ (resample with replacement);
 $\{\tilde{\mathbf{a}}_i\}_{i=1}^{N_{\text{samples}}} \leftarrow \{\tilde{\mathbf{a}}_i\}_{i=1}^{N_{\text{samples}}} + \sim \mathcal{N}(0, \sigma)$ (add random noise);
 $\sigma \leftarrow K\sigma$ (shrink sampling scale) ;
 $\hat{\mathbf{y}} = \arg \max(\{\tilde{p}_i\}, \{\tilde{\mathbf{a}}_i\})$

4.2.2 Langevin MCMC

We introduce a gradient-based MCMC training which uses gradient information for effective sampling and initializes chains from random noise for more mixing. Given an action datapoint a , let $E_{\theta}(a) \in \mathcal{R}$ be the energy function. The energy function would be represented by any function approximator but in our experiments conducted it is represented by a neural network with parameters θ . The energy function is used in tandem with the Boltzmann distribution $p_{\theta}(x) = \frac{\exp(-E_{\theta}(x))}{Z(\theta)}$, where $Z(\theta) = \int \exp(-E_{\theta}(x)) dx$ denotes the partition function. We further maintain a replay buffer of past samples and use them to initialize Langevin dynamics to allow mixing between chains. Specifically,

$${}^k \tilde{\mathbf{a}}_i^j = {}^{k-1} \tilde{\mathbf{a}}_i^j - \lambda \left(\frac{1}{2} \nabla_{\mathbf{a}} E_{\theta}(\mathbf{a}_i, {}^{k-1} \tilde{\mathbf{a}}_i^j) + \omega^k, \omega^k \sim \mathcal{N}(0, \sigma) \right)$$

where ${}^k \tilde{\mathbf{a}}_i^j$ means the j -th negative action sample in i -th batch of the k -th iteration. We let the above iterative procedure define a distribution q_{θ} such that $\tilde{\mathbf{a}}^k \sim q_{\theta}$. Welling and Teh [2011] showed that $q_{\theta} \rightarrow p_{\theta}$ almost surely as $k \rightarrow \infty$. Thus, samples are generated implicitly by the energy function E_{θ} as opposed to being explicitly generated by a neural network.

5 Experiments

5.1 Experiments setup

Task. We conduct our simulation experiments in PlasticineLab Huang et al. [2021], which provides a differentiable simulator that can simulate elastoplastic materials such as dough. Given a dough in a spherical shape, our task is to use a cylindrical roller to flatten the dough into a circular shape. We vary the initial and target dough locations, initial roller location, as well as the volume of the dough. An example of a trajectory in our simulation environment is shown at the top of Figure 1.

Evaluation metric. We use the normalized final Earth Mover’s Distance (EMD) as our performance metric in simulation, defined as:

$$\frac{D_{EMD}(P_0^d, P_g^d) - D_{EMD}(P_T^d, P_g^d)}{D_{EMD}(P_0^d, P_g^d)}$$

where P_0^d, P_T^d, P_g^d are the ground-truth dough point clouds at initialization, final timestep, and the target, respectively.

Baselines. We consider several baselines in simulation. First, we compare our method with a model-free RL baseline trained with point clouds as input: Soft Actor Critic (SAC) Haarnoja et al. [2017b]. Both the actor and the critic in SAC use the same inputs and the same encoder as our method. Specifically, we input the partial point cloud with a PointNet++ Qi et al. [2017] encoder and then perform standard actor-critic reinforcement learning with the latent feature. We train the SAC agent for 1 million timesteps and average the performance over 4 random seeds. Second, we compare with an explicit BC policy that directly outputs the control of the roller. Last, we compare the two different versions of the implicit BC method. One trained on random negative samples and the other trained with gradient-based, Langevin MCMC as in Florence et al. [2021] and Du and Mordatch [2019].

5.2 Implementation details

We use our trajectory optimizer to generate 150 demonstration trajectories uniformly sampled over 125 initial and target configurations. The trajectory optimizer runs Adam Optimizer Kingma and Ba [2014] for 1000 steps with a learning rate of 0.005. We then add Gaussian noise $\epsilon \sim \mathcal{N}(0, 0.01)$ to the demonstrations during to prevent overfitting in training. Our implicit model first maps the input point clouds to a compact state representation as a 1024-dimensional vector and then contact with the action to output an energy value.

5.3 Results

We evaluate all methods on 10 held-out configurations that have unseen initial and target states from training. First, we see that the trajectory optimizer (“Expert”) outperforms the SAC baseline by a wide margin, highlighting the advantage of a differentiable simulator when the state space is high-dimensional. We also see that both versions of the implicit policies trained on the demonstration data outperforms the explicit BC agent, showing again the benefit of learning an energy-based model over the state and action space. Last, utilizing the gradient information in both training and sampling, implicit BC with Langevin Dynamics is the best-performing method for this task.

To further demonstrate the generalization power of an implicit BC policy, we show the performance of implicit BC with Langevin Dynamics on both training and held-out configurations in Figure 4. Each point in the figure represents the performance of our policy on a specific configuration in the demonstration data. The policy is trained on points represented by circles and tested on the points represented by triangles. Although the test set contains more extreme values of dough size and target distance, our policy generalizes well to those configurations.

6 Conclusion

Compared to explicit regression model, implicit energy model can better approximate discontinuous, multi-valued function. In our dough rolling task, the optimal action is a two-stage process where the rolling pin need to first move down and contact with the dough, and then move back-and-forth

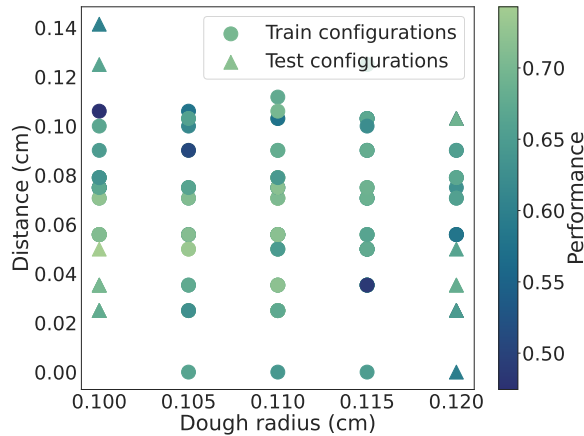


Figure 4: Performance of implicit BC with Langevin Dynamics over all configurations in the demonstration data. The policy is robust to unseen configurations (triangles).

horizontally to shape the dough into goal configuration. Our experiments suggest that implicit policy can better approximate this discontinuous trajectory and also better capture the multi-modality of actions, e.g., the rolling pin can move in different directions to flatten a dough.

For training the energy-based model, although random negative samples can provide useful learning signal, this procedure can be inefficient, especially when the dimension of the state space is large. In our case, we find that using a MCMC with Langevin Dynamics can effectively produce better negative samples and result in increase in performance and generalization.

Last, for inference, a derivative-based sampler is also more effective and yields better optimization results. This is related to the fact that our action space is relatively high dimensional as well. Similar phenomena can also be found in experiments in Florence et al. [2021].

References

- Y. Avigal, S. Paradis, and H. Zhang. 6-dof grasp planning using fast 3d reconstruction and grasp quality cnn. *arXiv preprint arXiv:2009.08618*, 2020.
- Y. Avigal, V. Satish, Z. Tam, H. Huang, H. Zhang, M. Danielczuk, J. Ichnowski, and K. Goldberg. Avplug: Approach vector planning for uncontact grasping amid clutter. In *2021 IEEE 17th international conference on automation science and engineering (CASE)*, pages 1140–1147. IEEE, 2021.
- Y. Deng, A. Bakhtin, M. Ott, A. Szlam, and M. Ranzato. Residual energy-based models for text generation. *arXiv preprint arXiv:2004.11714*, 2020.
- S. Devgon, J. Ichnowski, A. Balakrishna, H. Zhang, and K. Goldberg. Orienting novel 3d objects using self-supervised learning of rotation transforms. In *2020 IEEE 16th International Conference on Automation Science and Engineering (CASE)*, pages 1453–1460. IEEE, 2020.
- Y. Du and I. Mordatch. Implicit generation and modeling with energy based models. In H. Wallach, H. Larochelle, A. Beygelzimer, F. d'Alché-Buc, E. Fox, and R. Garnett, editors, *Advances in Neural Information Processing Systems*, volume 32. Curran Associates, Inc., 2019. URL <https://proceedings.neurips.cc/paper/2019/file/378a063b8fdb1db941e34f4bde584c7d-Paper.pdf>.
- Y. Du, S. Li, and I. Mordatch. Compositional visual generation with energy based models. *Advances in Neural Information Processing Systems*, 33:6637–6647, 2020.
- B. Eisner, H. Zhang, and D. Held. Flowbot3d: Learning 3d articulation flow to manipulate articulated objects. *arXiv preprint arXiv:2205.04382*, 2022.

- A. Elmquist, A. Young, T. Hansen, S. Ashokkumar, S. Caldararu, A. Dashora, I. Mahajan, H. Zhang, L. Fang, H. Shen, et al. Art/atk: A research platform for assessing and mitigating the sim-to-real gap in robotics and autonomous vehicle engineering. *arXiv preprint arXiv:2211.04886*, 2022.
- P. Florence, L. Manuelli, and R. Tedrake. Self-supervised correspondence in visuomotor policy learning. *IEEE Robotics and Automation Letters*, 5(2):492–499, 2019.
- P. Florence, C. Lynch, A. Zeng, O. A. Ramirez, A. Wahid, L. Downs, A. Wong, J. Lee, I. Mordatch, and J. Tompson. Implicit behavioral cloning. In *5th Annual Conference on Robot Learning*, 2021. URL <https://openreview.net/forum?id=rif3a5NAxU6>.
- J. Fu, A. Kumar, O. Nachum, G. Tucker, and S. Levine. D4rl: Datasets for deep data-driven reinforcement learning. *arXiv preprint arXiv:2004.07219*, 2020.
- F. K. Gustafsson, M. Danelljan, G. Bhat, and T. B. Schön. Energy-based models for deep probabilistic regression. In *European Conference on Computer Vision*, pages 325–343. Springer, 2020.
- T. Haarnoja, H. Tang, P. Abbeel, and S. Levine. Reinforcement learning with deep energy-based policies. In *International Conference on Machine Learning*, pages 1352–1361. PMLR, 2017a.
- T. Haarnoja, A. Zhou, P. Abbeel, and S. Levine. Soft actor-critic: Off-policy maximum entropy deep reinforcement learning with a stochastic actor. 2017b.
- T. Haarnoja, A. Zhou, K. Hartikainen, G. Tucker, S. Ha, J. Tan, V. Kumar, H. Zhu, A. Gupta, P. Abbeel, et al. Soft actor-critic algorithms and applications. *arXiv preprint arXiv:1812.05905*, 2018.
- E. Heiden, M. Macklin, Y. S. Narang, D. Fox, A. Garg, and F. Ramos. DiSEct: A Differentiable Simulation Engine for Autonomous Robotic Cutting. In *Proceedings of Robotics: Science and Systems*, Virtual, July 2021. doi: 10.15607/RSS.2021.XVII.067.
- J. Ho and S. Ermon. Generative adversarial imitation learning. *Advances in neural information processing systems*, 29, 2016.
- R. Hoque, D. Seita, A. Balakrishna, A. Ganapathi, A. Tanwani, N. Jamali, K. Yamane, S. Iba, and K. Goldberg. Visuospatial foresight for multi-step, multi-task fabric manipulation. 07 2020. doi: 10.15607/RSS.2020.XVI.034.
- Y. Hou, L. Liu, Q. Wei, X. Xu, and C. Chen. A novel ddpq method with prioritized experience replay. In *2017 IEEE international conference on systems, man, and cybernetics (SMC)*, pages 316–321. IEEE, 2017.
- Y. Hu, Y. Fang, Z. Ge, Z. Qu, Y. Zhu, A. Pradhana, and C. Jiang. A moving least squares material point method with displacement discontinuity and two-way rigid body coupling. *ACM Transactions on Graphics*, 37(4):150, 2018.
- Y. Hu, L. Anderson, T.-M. Li, Q. Sun, N. Carr, J. Ragan-Kelley, and F. Durand. DiffTaichi: Differentiable programming for physical simulation. *ICLR*, 2020.
- Z. Huang, Y. Hu, T. Du, S. Zhou, H. Su, J. B. Tenenbaum, and C. Gan. Plasticinelab: A soft-body manipulation benchmark with differentiable physics. In *International Conference on Learning Representations*, 2021. URL <https://openreview.net/forum?id=xCcdBRQEDW>.
- D. Jin, S. Karmalkar, H. Zhang, and L. Carlone. Multi-model 3d registration: Finding multiple moving objects in cluttered point clouds. *arXiv preprint arXiv:2402.10865*, 2024.
- D. Kingma and J. Ba. Adam: A method for stochastic optimization. *International Conference on Learning Representations*, 12 2014.
- I. Kostrikov, R. Fergus, J. Tompson, and O. Nachum. Offline reinforcement learning with fisher divergence critic regularization. In *International Conference on Machine Learning*, pages 5774–5783. PMLR, 2021.
- A. Kumar, A. Zhou, G. Tucker, and S. Levine. Conservative q-learning for offline reinforcement learning. *Advances in Neural Information Processing Systems*, 33:1179–1191, 2020.

- Y. LeCun, S. Chopra, R. Hadsell, M. Ranzato, and F. Huang. A tutorial on energy-based learning. *Predicting structured data*, 1(0), 2006.
- Y. Li, J. Wu, R. Tedrake, J. B. Tenenbaum, and A. Torralba. Learning particle dynamics for manipulating rigid bodies, deformable objects, and fluids. In *ICLR*, 2019.
- V. Lim, H. Huang, L. Y. Chen, J. Wang, J. Ichnowski, D. Seita, M. Laskey, and K. Goldberg. Planar robot casting with real2sim2real self-supervised learning. *arXiv preprint arXiv:2111.04814*, 2021.
- V. Lim, H. Huang, L. Y. Chen, J. Wang, J. Ichnowski, D. Seita, M. Laskey, and K. Goldberg. Real2sim2real: Self-supervised learning of physical single-step dynamic actions for planar robot casting. In *2022 International Conference on Robotics and Automation (ICRA)*, pages 8282–8289. IEEE, 2022.
- X. Lin, Y. Wang, J. Olkin, and D. Held. Softgym: Benchmarking deep reinforcement learning for deformable object manipulation. In *Conference on Robot Learning*, 2020.
- X. Lin, Y. Wang, Z. Huang, and D. Held. Learning visible connectivity dynamics for cloth smoothing. In *Conference on Robot Learning*, 2021.
- X. Ma, D. Hsu, and W. S. Lee. Learning latent graph dynamics for deformable object manipulation, 2021.
- C. Matl and R. Bajcsy. Deformable elasto-plastic object shaping using an elastic hand and model-based reinforcement learning. *2021 IEEE/RSJ International Conference on Intelligent Robots and Systems (IROS)*, pages 3955–3962, 2021.
- O. Nachum and M. Yang. Provable representation learning for imitation with contrastive fourier features. *Advances in Neural Information Processing Systems*, 34, 2021.
- A. v. d. Oord, Y. Li, and O. Vinyals. Representation learning with contrastive predictive coding. *arXiv preprint arXiv:1807.03748*, 2018.
- C. Pan, B. Okorn, H. Zhang, B. Eisner, and D. Held. Tax-pose: Task-specific cross-pose estimation for robot manipulation. *arXiv preprint arXiv:2211.09325*, 2022.
- X. B. Peng, P. Abbeel, S. Levine, and M. van de Panne. Deepmimic: Example-guided deep reinforcement learning of physics-based character skills. *ACM Transactions on Graphics (TOG)*, 37(4):1–14, 2018.
- D. Pomerleau. An autonomous land vehicle in a neural network. *Advances in Neural Information Processing Systems*, 1, 1998.
- C. R. Qi, L. Yi, H. Su, and L. J. Guibas. Pointnet++: Deep hierarchical feature learning on point sets in a metric space. *arXiv preprint arXiv:1706.02413*, 2017.
- S. Ross, G. Gordon, and D. Bagnell. A reduction of imitation learning and structured prediction to no-regret online learning. In *Proceedings of the fourteenth international conference on artificial intelligence and statistics*, pages 627–635. JMLR Workshop and Conference Proceedings, 2011.
- S. Shen, Z. Zhu, L. Fan, H. Zhang, and X. Wu. Diffclip: Leveraging stable diffusion for language grounded 3d classification. In *Proceedings of the IEEE/CVF Winter Conference on Applications of Computer Vision*, pages 3596–3605, 2024.
- K. C. Sim, F. Beaufays, A. Benard, D. Guliani, A. Kabel, N. Khare, T. Lucassen, P. Zadrazil, H. Zhang, L. Johnson, et al. Personalization of end-to-end speech recognition on mobile devices for named entities. In *2019 IEEE Automatic Speech Recognition and Understanding Workshop (ASRU)*, pages 23–30. IEEE, 2019.
- Y. Song and D. P. Kingma. How to train your energy-based models. *arXiv preprint arXiv:2101.03288*, 2021.
- R. Tedrake. *Underactuated Robotics*. 2022. URL <http://underactuated.mit.edu>.

- S. Teng, H. Zhang, D. Jin, A. Jasour, M. Ghaffari, and L. Carlone. Gmkf: Generalized moment kalman filter for polynomial systems with arbitrary noise. *arXiv preprint arXiv:2403.04712*, 2024.
- S. Tu, A. Robey, T. Zhang, and N. Matni. On the sample complexity of stability constrained imitation learning. *arXiv preprint arXiv:2102.09161*, 2021.
- M. Welling and Y. W. Teh. Bayesian learning via stochastic gradient langevin dynamics. In *Proceedings of the 28th international conference on machine learning (ICML-11)*, pages 681–688. Citeseer, 2011.
- Y. Yao, S. Deng, Z. Cao, H. Zhang, and L.-J. Deng. Apla: Additional perturbation for latent noise with adversarial training enables consistency. *arXiv preprint arXiv:2308.12605*, 2023.
- H. Zhang. Health diagnosis based on analysis of data captured by wearable technology devices. *International Journal of Advanced Science and Technology*, 95:89–96, 2016.
- H. Zhang, J. Ichnowski, Y. Avigal, J. Gonzales, I. Stoica, and K. Goldberg. Dex-net ar: Distributed deep grasp planning using a commodity cellphone and augmented reality app. In *2020 IEEE International Conference on Robotics and Automation (ICRA)*, pages 552–558. IEEE, 2020.
- H. Zhang, J. Ichnowski, D. Seita, J. Wang, H. Huang, and K. Goldberg. Robots of the lost arc: Self-supervised learning to dynamically manipulate fixed-endpoint cables. In *2021 IEEE International Conference on Robotics and Automation (ICRA)*, pages 4560–4567. IEEE, 2021.
- H. Zhang, B. Eisner, and D. Held. Flowbot++: Learning generalized articulated objects manipulation via articulation projection. *arXiv preprint arXiv:2306.12893*, 2023.
- T. Zhang, Z. McCarthy, O. Jow, D. Lee, X. Chen, K. Goldberg, and P. Abbeel. Deep imitation learning for complex manipulation tasks from virtual reality teleoperation. In *2018 IEEE International Conference on Robotics and Automation (ICRA)*, pages 5628–5635. IEEE, 2018.